 CMES, vol.13, no.1, pp.67-80, 2006

Weak Coupling of the Symmetric Galerkin BEM with FEM for Potential and Elastostatic Problems

R. Springhetti[1], G. Novati[1] and M. Margonari[2]

Abstract: With reference to potential and elastostatic problems, a BEM-FEM coupling procedure, based on the symmetric Galerkin version of the BEM, is developed; the continuity conditions at the interface of the BE and FE subdomains are enforced in weak form; the global linear system is characterized by a symmetric coefficient matrix. The procedure is numerically tested with reference first to 2D potential problems and successively to 3D elastoplastic problems (with plastic strains confined to the FE subdomain).

keyword: Finite element method, Symmetric Galerkin boundary element method, Weak coupling

1 Introduction

The finite element method (FEM) and the boundary element method (BEM) have relative benefits and limitations. For instance the FEM is well suited for inhomogeneous and anisotropic materials as well as for nonlinear constitutive behavior. Linear homogeneous problems defined on unbounded domains and/or in the presence of high stress concentration and possible displacement discontinuity loci can be analyzed more advantageously by integral equation approaches. There are many application contexts where a coupling between BEM and FEM is in principle very attractive: different parts of a structure can be modelled indipendently by FEM and BEM in order to exploit the advantages of both techniques. The first investigations on this idea date back to 1977 with the pioneering work of Zienkiewicz, Kelly and Bettes (1977) based on the collocational BEM. Two issues arose immediately: the difficulties related to the lack of symmetry in the coefficient matrix of the BEM and a proper enforcement of the matching conditions at the interface between BE and FE subdomains. Since then a large number of papers devoted to this topic have appeared: an extensive overview is given in Ganguly, Layton and Balakrishna (2000). Only few contributions on the BEM-FEM coupling are based on the Symmetric Galerkin BEM (the so-called SGBEM) in view of the more involved mathematical aspects related to this version. Contributions on SGBEM-FEM coupling procedures which report numerical applications are quite recent, especially in 3D, since efficient numerical tools for the evaluation of the singular double surface-integrals have been developed only in recent times, see Bonnet, Maier and Polizzotto (1998), Sauter and Schwab (1997), Li, Mear and Xiao (1998) and Frangi, Novati, Springhetti and Rovizzi (2002). On this subject it is worth mentioning the variationally based coupling procedure between FEM and an indirect version of the Galerkin BEM in Polizzotto and Zito (1994), the SGBEM macro elements to be coupled with FEM in Ganguly, Layton and Balakrishna (2000) and the FEM macro elements to be weakly coupled with SGBEM in Ganguly, Layton and Balakrishna (2004), both for 2D elasticity, the mixed-dimensional coupling of shell finite elements and 3D SGBEM domains in Haas and Kuhn (2003) and the applications to 3D fracture mechanics in Han and Atluri (2002) and Frangi and Novati (2003). In many papers the SGBEM subdomains, see for instance Haas and Kuhn (2003) and Ganguly, Layton and Balakrishna (2000), or the FEM subdomains, e.g. Ganguly, Layton and Balakrishna (2004), are handled as equivalent finite or boundary macro-elements respectively. On the contrary, the SGBEM-FEM alternating method proposed by Han and Atluri (2002) as well as the direct SGBEM-FEM procedure in Frangi and Novati (2003) involve all the unknowns from both FE and BE subdomains, thus allowing to preserve the nature of both FEM and SGBEM (i.e. these procedures are neither BE-based nor FE-based in the sense explained above).

A crucial aspect for coupled approaches is represented by the enforcement of the matching conditions (i.e. continuity of displacements and tractions) at the interface between the subdomains. When displacement continuity

[1] Department of Mechanical and Structural Engineering, University of Trento, Italy.
[2] Structural Department, EnginSoft, Bergamo, Italy.

is enforced in strong form, the BEs lying on the interface and the sides of the FEs adjacent to the interface should coincide, together with their nodes, as in Frangi and Novati (2003). On the other hand, if the kinematic continuity condition is enforced in weak form, the matching of the two discretizations at the interface is no longer necessary, with an evident flexibility gain in the meshing process. This approach permits the integration of independently discretized models possibly coming from different sources. Specific relaxation algorithms have been used by some authors to achieve this goal (see e.g. Elleithy and Tanaka (2003) for BEM-FEM coupling); a non-matching node coupling of SGBEM and FEM is developed in Ganguly, Layton and Balakrishna (2004) in the context of a BE-based approach. In the fracture mechanics context a coupling approach which preserves the independence of the FE and BE meshes is the so-called hybrid surface-integral-finite-element technique, see Keat, Annigeri and Cleary (1988), Han and Atluri (2002) and Forth and Staroselsky (2005).

The present contribution addresses a SGBEM-FEM coupling procedure characterized by a weak enforcement of the displacement matching conditions on the interface. The proposed procedure which was simply outlined (but not numerically tested) in Frangi and Novati (2003), leads to a final equation system with symmetric matrix and allows the adoption of completely independent discretizations for the BE and the FE subdomains. The paper is organized as follows. Sections 2 and 4 illustrate the coupling procedure for the 2D potential problem and 3D elasticity, respectively. While a non-regularized version of the SGBEM is considered in Section 2 (with double integrations performed analitically for straight BEs), the regularized approach is adopted in Section 4 and the relevant weakly-singular double surface-integrals are evaluated numerically as described in Frangi, Novati, Springhetti and Rovizzi (2002). Section 3 provides a numerical verification of the coupling procedure with reference to 2D potential problems. Section 5 describes a variational basis for the proposed coupling procedure with reference to elasticity. Finally section 6 illustrates some numerical tests for elastoplastic problems characterized by a limited spread of plastic strains (within the FE subdomain).

2 Weak coupling for potential problems in 2D

The SGBEM-FEM coupling procedure will be first illustrated for the simple context of the Laplace equation on 2D domains. Let Ω denote a body of boundary Γ with prescribed potential $\overline{u}$ on the boundary portion Γ_u and assigned flux $\overline{q}$ on the complementary portion Γ_q ($\Gamma = \Gamma_u \cup \Gamma_q$) (see Fig. 1).

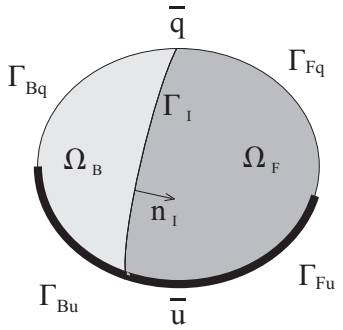

Figure 1 : Notation

The domain Ω is subdivided into two subdomains Ω_B and Ω_F. The approximate solution is sought adopting the integral equations of the symmetric approach over Ω_B (primary variables being the boundary potential u and flux q) and the FE equations over Ω_F (primary variables being the potential u^F). The matching conditions at the interface between Ω_B and Ω_F, denoted by Γ_I, are expressed in strong form as:

$$u^F = u \quad \text{and} \quad \nabla u^F \cdot \mathbf{n}_I + q = 0 \quad \text{on } \Gamma_I. \tag{1}$$

Here $\mathbf{n}_I$ denotes the unit vector normal to Γ_I directed outward from Ω_B, while in what follows $\mathbf{n}$ will refer to the outward unit vector normal to the boundary Γ. With the same notation introduced above, we denote as Γ_{Bu} and Γ_{Bq} the portions of the exterior boundary Γ_B of Ω_B ($\Gamma_B = \Gamma_{Bu} \cup \Gamma_{Bq}$) where potential and flux are prescribed: $u = \overline{u}$ on Γ_{Bu} and $q = \overline{q}$ on Γ_{Bq}. Analogously Γ_{Fu} and Γ_{Fq} denote the corresponding portions of the exterior boundary Γ_F of Ω_F ($\Gamma_F = \Gamma_{Fu} \cup \Gamma_{Fq}$): $u^F = \overline{u}$ on Γ_{Fu} and $\nabla u^F \cdot \mathbf{n} = \overline{q}$ on Γ_{Fq}. Obviously $\Gamma_u = \Gamma_{Fu} \cup \Gamma_{Bu}$ and $\Gamma_q = \Gamma_{Fq} \cup \Gamma_{Bq}$.

On the boundary $\overline{\Gamma}_B = \Gamma_B \cup \Gamma_I$ of domain Ω_B the following integral equations are enforced (see Sirtori, Maier, Novati and Miccoli (1992)), in which the primary variables are both the potential u and the flux q:

- potential equation for $\tilde{\mathbf{x}} \in \tilde{\Gamma}_I$

$$\int_{\tilde{\Gamma}_I} \tilde{f}(\tilde{\mathbf{x}}) \int_{\overline{\Gamma}_B} [G^{uu}(\tilde{\mathbf{x}},\mathbf{x}) q(\mathbf{x}) - G^{uq}(\tilde{\mathbf{x}},\mathbf{x}) u(\mathbf{x})]\, d\Gamma d\tilde{\Gamma} = 0 \quad (2)$$

- potential equation for $\tilde{\mathbf{x}} \in \tilde{\Gamma}_{Bu}$

$$\int_{\tilde{\Gamma}_{Bu}} \tilde{f}(\tilde{\mathbf{x}}) \int_{\overline{\Gamma}_B} [G^{uu}(\tilde{\mathbf{x}},\mathbf{x}) q(\mathbf{x}) - G^{uq}(\tilde{\mathbf{x}},\mathbf{x}) u(\mathbf{x})]\, d\Gamma d\tilde{\Gamma} = 0 \quad (3)$$

- flux equation for $\tilde{\mathbf{x}} \in \tilde{\Gamma}_I$

$$\int_{\tilde{\Gamma}_I} \tilde{d}(\tilde{\mathbf{x}}) \int_{\overline{\Gamma}_B} [G^{qu}(\tilde{\mathbf{x}},\mathbf{x}) q(\mathbf{x}) - G^{qq}(\tilde{\mathbf{x}},\mathbf{x}) u(\mathbf{x})]\, d\Gamma d\tilde{\Gamma} = 0 \quad (4)$$

- flux equation for $\tilde{\mathbf{x}} \in \tilde{\Gamma}_{Bq}$

$$\int_{\tilde{\Gamma}_{Bq}} \tilde{d}(\tilde{\mathbf{x}}) \int_{\overline{\Gamma}_B} [G^{qu}(\tilde{\mathbf{x}},\mathbf{x}) q(\mathbf{x}) - G^{qq}(\tilde{\mathbf{x}},\mathbf{x}) u(\mathbf{x})\, d\Gamma] d\tilde{\Gamma} = 0. \quad (5)$$

The above equations involve an auxiliary line $\tilde{\overline{\Gamma}}_B$ running outside Ω_B, whose points $\tilde{\mathbf{x}}$ are in a one-to-one correspondence with the points $\mathbf{x}$ on $\overline{\Gamma}_B$. Obviously $\tilde{\overline{\Gamma}}_B = \tilde{\Gamma}_{Bu} \cup \tilde{\Gamma}_{Bq} \cup \tilde{\Gamma}_I$, each of these line portions corresponding to the analogous portion on $\overline{\Gamma}_B$. Functions $\tilde{d}(\tilde{\mathbf{x}})$ and $\tilde{f}(\tilde{\mathbf{x}})$ represent fictitious potential and flux discontinuities across $\tilde{\overline{\Gamma}}_B$ respectively, while symbol $G^{ij}(\tilde{\mathbf{x}},\mathbf{x})$ denotes the influence functions associated to the Laplace equation. More specifically, $G^{ij}(\tilde{\mathbf{x}},\mathbf{x})$ represents the effect j (potential if $j=u$ or flux if $j=q$) at point $\mathbf{x}$ generated by a unit concentrated "load" which acts at $\tilde{\mathbf{x}}$ and whose nature is identified by index i through a conjugation rule in the virtual work sense (i.e. $i=u$ and $i=q$ denote a concentrated domain-source and a concentrated potential discontinuity, respectively). Note that the potential and the flux equations contain strongly-singular and hyper-singular contributions respectively; as an alternative, a strongly-singular version of the flux equation is available in literature, see Han and Atluri (2003).

Concomitantly, the Laplace equation is enforced in weak form on subdomain Ω_F, introducing a test function $\tilde{u}^F$:

$$\int_{\Omega_F} \nabla \tilde{u}^F(\mathbf{x}) \cdot \nabla u^F(\mathbf{x}) d\Omega = \int_{\Gamma_{Fq}} \tilde{u}^F(\mathbf{x})\, \overline{q}(\mathbf{x})\, d\Gamma + \int_{\Gamma_I} \tilde{u}^F(\mathbf{x})\, \nabla u^F(\mathbf{x}) \cdot \mathbf{n}_I(\mathbf{x})\, d\Gamma, \quad (6)$$

where u^F and $\tilde{u}^F$ are assumed to satisfy the actual and the homogeneous boundary conditions on Γ_{Fu} respectively.

In the present approach, the matching conditions at the interface Γ_I, eqs. (1), are enforced in weak form using as weight functions the auxiliary fields $\tilde{f}$ and $\tilde{u}^F$ previously introduced:

$$\int_{\Gamma_I} \tilde{f}(\mathbf{x}) [u^F(\mathbf{x}) - u(\mathbf{x})]\, d\Gamma = 0 \quad (7)$$

$$\int_{\Gamma_I} \tilde{u}^F(\mathbf{x}) [\nabla u^F(\mathbf{x}) \cdot \mathbf{n}_I(\mathbf{x}) + q(\mathbf{x})]\, d\Gamma = 0. \quad (8)$$

Let us now discretize along the lines $\overline{\Gamma}_B$ and $\tilde{\overline{\Gamma}}_B$ the primary fields involved in the integral equations:

$$u(\mathbf{x}) = \left[\mathbf{N}_u(\mathbf{x})\right]^t \mathbf{U}, \qquad \tilde{d}(\tilde{\mathbf{x}}) = \left[\mathbf{N}_u(\tilde{\mathbf{x}})\right]^t \tilde{\mathbf{D}}, \quad (9)$$

$$q(\mathbf{x}) = \left[\mathbf{N}_q(\mathbf{x})\right]^t \mathbf{Q}, \qquad \tilde{f}(\tilde{\mathbf{x}}) = \left[\mathbf{N}_q(\tilde{\mathbf{x}})\right]^t \tilde{\mathbf{F}} \quad (10)$$

where $\mathbf{N}_i$ $(i = u, q)$ denote vectors of shape functions, while $\mathbf{U}$, $\mathbf{Q}$, $\tilde{\mathbf{D}}$ and $\tilde{\mathbf{F}}$ collect the nodal values of the modelled fields. In the spirit of a Galerkin approach, the shape functions are chosen to be the same for actual and auxiliary fields of the same nature. Note that the modelled potential has to be continuous, while there are no requirements on the modeling of the flux. The discretization of subdomain Ω_F into finite elements is also introduced, with the potential u^F and the auxiliary field $\tilde{u}^F$ modelled as follows through the shape functions collected in vector $\mathbf{N}_u^F$:

$$u^F(\mathbf{x}) = \left[\mathbf{N}_u^F(\mathbf{x})\right]^t \mathbf{U}^F \qquad \tilde{u}^F(\mathbf{x}) = \left[\mathbf{N}_u^F(\mathbf{x})\right]^t \tilde{\mathbf{U}}^F. \quad (11)$$

The limiting versions of eqs. (2)-(5) represent the boundary integral equations of the SGBEM. In the case of straight elements and simple shape functions (here linear interpolations have been adopted) the double integrals emerging after the discretization of eqs. (2)-(5) can be evaluated analytically for $\tilde{\overline{\Gamma}}_B$ distinct from $\overline{\Gamma}_B$, together with their limiting values for $\tilde{\overline{\Gamma}}_B \to \overline{\Gamma}_B$, as shown in Sirtori, Maier, Novati and Miccoli (1992). The SGBEM discretized equations read:

$$\left[\tilde{\mathbf{F}}^I\right]^t \left(\mathbf{G}_{II}^{uu}\mathbf{Q}^I + \mathbf{G}_{Iu}^{uu}\mathbf{Q}^u - \mathbf{G}_{II}^{uq}\mathbf{U}^I - \mathbf{G}_{Iq}^{uq}\mathbf{U}^q - \mathbf{G}_{Iu}^{uq}\overline{\mathbf{U}} + \mathbf{G}_{Iq}^{uu}\overline{\mathbf{Q}}\right) = 0, \quad \forall\, \tilde{\mathbf{F}}^I \quad (12)$$

$$\left[\tilde{\mathbf{F}}^u\right]^t\left(\mathbf{G}_{uI}^{uu}\mathbf{Q}^I+\mathbf{G}_{uu}^{uu}\mathbf{Q}^u-\mathbf{G}_{uI}^{uq}\mathbf{U}^I-\mathbf{G}_{uq}^{uq}\mathbf{U}^q-\mathbf{G}_{uu}^{uq}\overline{\mathbf{U}}+\mathbf{G}_{uq}^{uu}\overline{\mathbf{Q}}\right)=0,\quad\forall\,\tilde{\mathbf{F}}^u \tag{13}$$

$$\left[\tilde{\mathbf{D}}^I\right]^t\left(\mathbf{G}_{II}^{qu}\mathbf{Q}^I+\mathbf{G}_{Iu}^{qu}\mathbf{Q}^u-\mathbf{G}_{II}^{qq}\mathbf{U}^I-\mathbf{G}_{Iq}^{qq}\mathbf{U}^q-\mathbf{G}_{Iu}^{qq}\overline{\mathbf{U}}+\mathbf{G}_{Iq}^{qu}\overline{\mathbf{Q}}\right)=0,\quad\forall\,\tilde{\mathbf{D}}^I \tag{14}$$

$$\left[\tilde{\mathbf{D}}^q\right]^t\left(\mathbf{G}_{qI}^{qu}\mathbf{Q}^I+\mathbf{G}_{qu}^{qu}\mathbf{Q}^u-\mathbf{G}_{qI}^{qq}\mathbf{U}^I-\mathbf{G}_{qq}^{qq}\mathbf{U}^q-\mathbf{G}_{qu}^{qq}\overline{\mathbf{U}}+\mathbf{G}_{qq}^{qu}\overline{\mathbf{Q}}\right)=0,\quad\forall\,\tilde{\mathbf{D}}^q. \tag{15}$$

The definition of matrices $\mathbf{G}_{hk}^{ij}$ is straightforward; superscripts i and j $(i,j=u,q)$ play the same role as in the kernels; subscripts h and k $(h,k=u,q,I)$ denote, respectively, the boundary portions where the fictitious sources are located and where their effects are integrated, e.g.

$$\mathbf{G}_{II}^{uq}=\int_{\Gamma_I}\int_{\Gamma_I}\mathbf{N}_q(\tilde{\mathbf{x}})\,G^{uq}(\tilde{\mathbf{x}},\mathbf{x})\left[\mathbf{N}_u(\mathbf{x})\right]^t d\Gamma d\Gamma. \tag{16}$$

Vectors $\mathbf{U}^I$, $\mathbf{Q}^I$, $\mathbf{U}^q$, $\mathbf{Q}^u$ represent the unknown nodal values of u and q on the portions Γ_I, Γ_{Bq} and Γ_{Bu} respectively, while $\overline{\mathbf{U}}$ and $\overline{\mathbf{Q}}$ are the known nodal values along Γ_{Bu} and Γ_{Bq} respectively.

In view of the reciprocity properties enjoyed by the kernels $\mathbf{G}^{ij}$ and of the choice of the shape functions in the Galerkin fashion, the following reciprocity properties hold for matrices $\mathbf{G}_{hk}^{ij}$, see Sirtori, Maier, Novati and Miccoli (1992):

$$\mathbf{G}_{hk}^{ij}=\left[\mathbf{G}_{kh}^{ji}\right]^t\qquad\text{if } i=j \text{ or if } i\neq j \text{ and } h\neq k \tag{17}$$

$$\mathbf{G}_{II}^{uq}=\left[\mathbf{G}_{II}^{qu}\right]^t+\int_{\Gamma_I}\mathbf{N}_q(\mathbf{x})\left[\mathbf{N}_u(\mathbf{x})\right]^t d\Gamma \tag{18}$$

With the aim of generating a symmetric overall equation system, the following steps are taken. Equation (12) is transformed by expressing $\mathbf{G}_{II}^{uq}$ through eq. (18) and using the weak form of the potential continuity condition, eq. (7), in discretized form. Hence the final version of eq. (12) reads:

$$\left[\tilde{\mathbf{F}}^I\right]^t\left(-\left[\mathbf{J}_{uI}\right]^t\mathbf{U}^F+\mathbf{G}_{II}^{uu}\mathbf{Q}^I+\mathbf{G}_{Iu}^{uu}\mathbf{Q}^u-\left[\mathbf{G}_{II}^{qu}\right]^t\mathbf{U}^I-\mathbf{G}_{Iq}^{uq}\mathbf{U}^q-\mathbf{G}_{Iu}^{uq}\overline{\mathbf{U}}+\mathbf{G}_{Iq}^{uu}\overline{\mathbf{Q}}\right)=0,\quad\forall\,\tilde{\mathbf{F}}^I. \tag{19}$$

Matrix $\mathbf{J}_{uI}$ involves the BE shape functions for the flux and the FE shape functions for the potential (see Fig. 2) and reads:

$$\mathbf{J}_{uI}=\int_{\Gamma_I}\mathbf{N}_u^F(\mathbf{x})\left[\mathbf{N}_q(\mathbf{x})\right]^t d\Gamma. \tag{20}$$

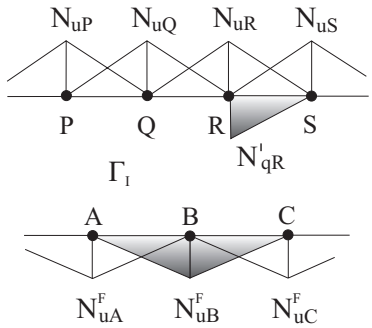

Figure 2 : Shape functions involved in the evaluation of matrix $\mathbf{J}_{uI}$

As for the FE equations, the flux continuity condition, eq. (8), is now plugged into eq. (6), which takes the form:

$$\int_{\Omega_F}\nabla\tilde{u}^F(\mathbf{x})\cdot\nabla u^F(\mathbf{x})\,d\Omega+\int_{\Gamma_I}\tilde{u}^F(\mathbf{x})\,q(\mathbf{x})\,d\Gamma=\int_{\Gamma_{Fq}}\tilde{u}^F(\mathbf{x})\,\overline{q}(\mathbf{x})\,d\Gamma. \tag{21}$$

Upon discretization, eq. (21) can be rewritten as follows, taking into account the BE modeling of the flux q on Γ_I:

$$\left[\tilde{\mathbf{U}}^F\right]^t\left(\mathbf{K}\,\mathbf{U}^F+\mathbf{J}_{uI}\,\mathbf{Q}^I-\overline{\mathbf{Q}}^F\right)=0,\quad\forall\tilde{\mathbf{U}}^F. \tag{22}$$

Here $\mathbf{K}$ represents the stiffness matrix, while $\overline{\mathbf{Q}}^F$ are the equivalent nodal loads.

Collecting eqs. (22), (19), (13)-(15) and enforcing them $\forall\tilde{\mathbf{U}}^F$, $\tilde{\mathbf{F}}^I$, $\tilde{\mathbf{D}}^I$, $\tilde{\mathbf{F}}^u$, $\tilde{\mathbf{D}}^q$, the global equation system is finally generated, i.e. in matrix notation:

$$\begin{bmatrix}\mathbf{K}&\mathbf{J}_{uI}&\mathbf{0}&\mathbf{0}&\mathbf{0}\\ \left[\mathbf{J}_{uI}\right]^t&-\mathbf{G}_{II}^{uu}&-\mathbf{G}_{Iu}^{uu}&\left[\mathbf{G}_{II}^{qu}\right]^t&\mathbf{G}_{Iq}^{uq}\\ \mathbf{0}&-\mathbf{G}_{uI}^{uu}&-\mathbf{G}_{uu}^{uu}&\mathbf{G}_{uI}^{uq}&\mathbf{G}_{uq}^{uq}\\ \mathbf{0}&\mathbf{G}_{II}^{qu}&\mathbf{G}_{Iu}^{qu}&-\mathbf{G}_{II}^{qq}&-\mathbf{G}_{Iq}^{qq}\\ \mathbf{0}&\mathbf{G}_{qI}^{qu}&\mathbf{G}_{qu}^{qu}&-\mathbf{G}_{qI}^{qq}&-\mathbf{G}_{qq}^{qq}\end{bmatrix}\left\{\begin{array}{c}\mathbf{U}^F\\ \mathbf{Q}^I\\ \mathbf{Q}^u\\ \mathbf{U}^I\\ \mathbf{U}^q\end{array}\right\}=\mathbf{P} \tag{23}$$

with data vector **P**:

$$\mathbf{P} = \left\{ \begin{array}{c} \overline{\mathbf{Q}}^F \\ -\mathbf{G}_{Iu}^{uq}\overline{\mathbf{U}} + \mathbf{G}_{Iq}^{uu}\overline{\mathbf{Q}} \\ -\mathbf{G}_{uu}^{uq}\overline{\mathbf{U}} + \mathbf{G}_{uq}^{uu}\overline{\mathbf{Q}} \\ \mathbf{G}_{Iu}^{qq}\overline{\mathbf{U}} - \mathbf{G}_{Iq}^{qu}\overline{\mathbf{Q}} \\ \mathbf{G}_{qu}^{qq}\overline{\mathbf{U}} - \mathbf{G}_{qq}^{qu}\overline{\mathbf{Q}} \end{array} \right\}. \tag{24}$$

The symmetry of the coefficient matrix is evident.

3 Numerical validation for 2D potential problems

The procedure illustrated above has been implemented into a computer code. Straight BEs are adopted with linear modeling for the potential and the flux, the latter being discontinuous across elements. Bilinear four-noded FEs are employed. Two test problems, denoted by *A* and *B*, have been considered; both are governed by the Laplace equation and refer to the simple geometry and to the boundary condition types depicted in Fig. 3. FE and BE modeling are used in the two subdomains Ω_F and Ω_B respectively.

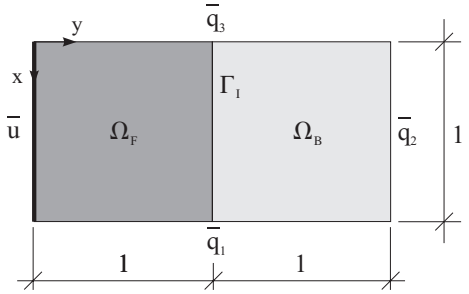

Figure 3 : Test problem

In Problem *A* the boundary conditions are the following: $\overline{u} = 0$, $\overline{q}_1 = \overline{q}_3 = 0$, $\overline{q}_2 = 1$; hence the exact solution is $u = y$. In Problem *B* the boundary conditions are chosen as the boundary potential and flux subordinated to the following harmonic potential

$$u(x,y) = x^3 + 3x^2y - 3xy^2 - y^3 - 5,$$

hence representing the exact solution to Problem *B*.

Problem *A* is solved using the simple mesh of Fig. 4, consisting of 4 identical FEs and 6 BEs. Note that in this problem there is no modeling error (since the shape functions adopted allow to capture the exact solution) and no approximation in the evaluation of the SGBEM double integrals (computed analytically); besides, in this case, the weak form enforcement of the interface conditions imply the satisfaction of their strong form version. Therefore only round-off errors are expected in the numerical solution. This turns out to be confirmed by the numerical test carried out, which thus represents a first validation of the proposed procedure.

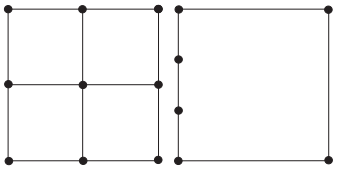

Figure 4 : Discretization for Problem *A*

Problem *B* is solved using two different meshes:

- mesh 1: 16 equal FEs in Ω_F and 12 equal BEs (3 along each side of $\overline{\Gamma}_B$);
- mesh 2: 64 equal FEs in Ω_F and 24 equal BEs (6 along each side of $\overline{\Gamma}_B$).

The numerical results are summarized in Tab. 1 in terms of percentage errors in the computed nodal values for the potential and the flux. The table lists also the residuals of the discretized version of eq. (7), which quantify the degree of fulfilment of the potential continuity equation along Γ_I. Such residuals have been compared to those relevant to the potential boundary integral eqs. (13) enforced on Γ_B, taking into account the boundary solution determined on Γ_B (note that the potential equations are not used in the SGBEM-FEM procedure for the problem at hand since $\Gamma_{Bu} = \emptyset$). As shown in Tab. 1, the residuals on Γ_I and Γ_{Bu} turn out to be comparable and this

corroborates the validity of the proposed approach.

		mesh 1	mesh 2
% error in the potentials on $\overline{\Gamma}_B$	max	2.5	0.8
	aver.	1.1	0.3
% error in the fluxes on $\overline{\Gamma}_B$	max	7.0	2.2
	aver.	3.7	0.1
% error in the potentials on Ω_F	max	0.9	0.2
	aver.	0.3	0.1
residuals of eq. (7) on Γ_I	max	$8.0\cdot10^{-3}$	10^{-3}
	aver.	$4.0\cdot10^{-3}$	$3.0\cdot10^{-4}$
residuals of eq. (13) on Γ_B	max	$1.2\cdot10^{-2}$	$1.4\cdot10^{-3}$
	aver.	$5.0\cdot10^{-3}$	$3.9\cdot10^{-4}$

Table 1: Errors in the numerical solution for Problem B

4 Weak coupling for elasticity in 3D

The same notation already introduced for the potential problem is adopted here, but reference is now to 3D elastic problems. The boundary Γ of the body Ω is constrained along its portion Γ_u and loaded upon Γ_q. The subdomains Ω_B and Ω_F are introduced, where the modeling consists of BEs and displacement-based FEs respectively. The boundary conditions for the displacements $\mathbf{u}$ and the tractions $\mathbf{q}$ on Γ_B, as well as for the displacements $\mathbf{u}^F$ and the tractions on Γ_F, read:

$$\mathbf{u}=\overline{\mathbf{u}} \ \text{ on } \Gamma_{Bu} \quad \text{and} \quad \mathbf{q}=\overline{\mathbf{q}} \ \text{ on } \Gamma_{Bq}$$
$$\mathbf{u}^F=\overline{\mathbf{u}} \ \text{ on } \Gamma_{Fu} \quad \text{and} \quad \sigma^F\mathbf{n}=\overline{\mathbf{q}} \ \text{ on } \Gamma_{Fq}.$$

Here $\sigma^F=\mathbf{E}:\nabla\mathbf{u}^F$ represents the stress tensor associated to $\mathbf{u}^F$, $\mathbf{E}$ being the conventional linear elastic tensor.

The continuity and equilibrium conditions between Ω_B and Ω_F along Γ_I read (strong form):

$$\mathbf{u}^F=\mathbf{u} \quad \text{and} \quad \sigma^F\mathbf{n}_I+\mathbf{q}=\mathbf{0} \ \text{ on } \Gamma_I. \tag{25}$$

The boundary integral equations on $\overline{\Gamma}_B$, which in principle involve hypersingular, strongly singular and weakly singular integrals, are written here in a regularized form, see Bonnet, Maier and Polizzotto (1998), with at most weakly singular integrals.

- displacement equation for $\tilde{\mathbf{x}}\in\Gamma_I$

$$\frac{1}{2}\int_{\Gamma_I}\tilde{\mathbf{f}}(\mathbf{x})\cdot\mathbf{u}(\mathbf{x})\,d\Gamma=\int_{\Gamma_I}\int_{\overline{\Gamma}_B}\tilde{\mathbf{f}}(\tilde{\mathbf{x}})\cdot\Big[\mathbf{G}^{uu}(\tilde{\mathbf{x}},\mathbf{x})\,\mathbf{q}(\mathbf{x})+\frac{\nabla r\cdot\mathbf{n}(\mathbf{x})}{4\pi r^2}\mathbf{u}(\mathbf{x})+\mathbf{G}^{u\varphi}(\tilde{\mathbf{x}},\mathbf{x}):\mathbf{R}[\mathbf{u}](\mathbf{x})\Big]\,d\Gamma d\Gamma \tag{26}$$

- displacement equation for $\tilde{\mathbf{x}}\in\Gamma_{Bu}$

$$\frac{1}{2}\int_{\Gamma_{Bu}}\tilde{\mathbf{f}}(\mathbf{x})\cdot\mathbf{u}(\mathbf{x})\,d\Gamma=\int_{\Gamma_{Bu}}\int_{\overline{\Gamma}_B}\tilde{\mathbf{f}}(\tilde{\mathbf{x}})\cdot\Big[\mathbf{G}^{uu}(\tilde{\mathbf{x}},\mathbf{x})\,\mathbf{q}(\mathbf{x})+\frac{\nabla r\cdot\mathbf{n}(\mathbf{x})}{4\pi r^2}\mathbf{u}(\mathbf{x})+\mathbf{G}^{u\varphi}(\tilde{\mathbf{x}},\mathbf{x}):\mathbf{R}[\mathbf{u}](\mathbf{x})\Big]\,d\Gamma d\Gamma \tag{27}$$

- traction equation for $\tilde{\mathbf{x}}\in\Gamma_I$

$$\frac{1}{2}\int_{\Gamma_I}\tilde{\mathbf{d}}(\mathbf{x})\cdot\mathbf{q}(\mathbf{x})\,d\Gamma=-\int_{\Gamma_I}\int_{\overline{\Gamma}_B}\Big\{\frac{\tilde{\nabla}r\cdot\tilde{\mathbf{n}}(\tilde{\mathbf{x}})}{4\pi r^2}\,\tilde{\mathbf{d}}(\tilde{\mathbf{x}})\cdot\mathbf{q}(\mathbf{x})+\tilde{\mathbf{R}}[\tilde{\mathbf{d}}](\tilde{\mathbf{x}}):\big[\mathbf{G}^{\varphi u}(\tilde{\mathbf{x}},\mathbf{x})\,\mathbf{q}(\mathbf{x})+\mathbf{G}^{\varphi\varphi}(\tilde{\mathbf{x}},\mathbf{x}):\mathbf{R}[\mathbf{u}](\mathbf{x})\big]\Big\}\,d\Gamma d\Gamma \tag{28}$$

- traction equation for $\tilde{\mathbf{x}}\in\Gamma_{Bq}$

$$\frac{1}{2}\int_{\Gamma_{Bq}}\tilde{\mathbf{d}}(\mathbf{x})\cdot\mathbf{q}(\mathbf{x})\,d\Gamma=-\int_{\Gamma_{Bq}}\int_{\overline{\Gamma}_B}\Big\{\frac{\tilde{\nabla}r\cdot\tilde{\mathbf{n}}(\tilde{\mathbf{x}})}{4\pi r^2}\,\tilde{\mathbf{d}}(\tilde{\mathbf{x}})\cdot\mathbf{q}(\mathbf{x})+\tilde{\mathbf{R}}[\tilde{\mathbf{d}}](\tilde{\mathbf{x}}):\big[\mathbf{G}^{\varphi u}(\tilde{\mathbf{x}},\mathbf{x})\,\mathbf{q}(\mathbf{x})+\mathbf{G}^{\varphi\varphi}(\tilde{\mathbf{x}},\mathbf{x}):\mathbf{R}[\mathbf{u}](\mathbf{x})\big]\Big\}\,d\Gamma d\Gamma. \tag{29}$$

The gradient operators and the surface rotors are defined according to the notation:

$$[\nabla r]_k=r_{,k}=\partial r/\partial x_k, \qquad [\tilde{\nabla}r]_k=r_{,\tilde{k}}=\partial r/\partial\tilde{x}_k,$$

$$\big[\mathbf{R}[\mathbf{u}](\mathbf{x})\big]_{ij}=R_j[u_i](\mathbf{x})=e_{hkj}n_h(\mathbf{x})u_{i,k}(\mathbf{x}),$$

$$\big[\tilde{\mathbf{R}}[\tilde{\mathbf{d}}](\tilde{\mathbf{x}})\big]_{ij}=\tilde{R}_j[\tilde{d}_i](\tilde{\mathbf{x}})=e_{hkj}\tilde{n}_h(\tilde{\mathbf{x}})\tilde{d}_{i,\tilde{k}}(\tilde{\mathbf{x}}),$$

e_{ijk} being the Ricci permutation symbol. The symbol : denotes a double contraction of successive indices, i.e., if A and B are third and second order tensors respectively, $[A:B]_i=A_{ijh}B_{jh}$. The explicit expression for the kernels are obtained by means of the regularization procedure from the fundamental solutions for 3D elasticity and read:

$$G^{uu}_{ij}(\tilde{\mathbf{x}},\mathbf{x})=\frac{1}{16\pi\mu(1-\nu)}\frac{1}{r}\left[(3-4\nu)\delta_{ij}+r_{,i}r_{,j}\right] \tag{30}$$

$$G^{u\varphi}_{ijk}(\tilde{\mathbf{x}},\mathbf{x})=\frac{1}{8\pi(1-\nu)r}\left[(1-2\nu)\,e_{ijk}-e_{ihk}r_{,h}r_{,j}\right] \tag{31}$$

$$G_{ijk}^{\varphi u} = \frac{1}{8\pi(1-\nu)r}\left[(1-2\nu)\,e_{ijk} - e_{khj}r_{,h}r_{,i}\right] \tag{32}$$

$$G_{ijhk}^{\varphi\varphi} = -\frac{\mu}{8\pi}\frac{1}{r}\left(\delta_{ab} - r_{,a}\,r_{,b}\right)e_{iac}e_{jbd}\left[\frac{2\nu}{1-\nu}\delta_{ch}\delta_{dk} + \delta_{cd}\delta_{hk} + \delta_{ck}\delta_{hd}\right] \tag{33}$$

where δ_{ij} represents the Kronecker delta. The integral contribution, which do not involve any kernel, are weakly singular as well since, on a smooth surface, $r_{,i}n_i/r^2$ is $O(1/r)$, as $r \to 0$. All the weakly singular integrals involved can be evaluated numerically as shown e.g. in Frangi, Novati, Springhetti and Rovizzi (2002).

On subdomain Ω_F the displacements $\mathbf{u}^F$ are sought, *a priori* satisfying the boundary kinematical conditions, such that:

$$\int_{\Omega_F} \tilde{\varepsilon}^F(\mathbf{x}) : \sigma^F(\mathbf{x})\,d\Omega = \int_{\Gamma_{Fq}} \tilde{\mathbf{u}}^F(\mathbf{x}) \cdot \overline{\mathbf{q}}(\mathbf{x})\,d\Gamma + \int_{\Gamma_I} \tilde{\mathbf{u}}^F(\mathbf{x}) \cdot \sigma^F(\mathbf{x})\,\mathbf{n}(\mathbf{x})\,d\Gamma. \tag{34}$$

The developments already illustrated in section 2 are now paralleled here below. First the interface conditions, eqs. (25), are rewritten in weak form:

$$\int_{\Gamma_I} \tilde{\mathbf{f}}(\mathbf{x}) \cdot [\mathbf{u}^F(\mathbf{x}) - \mathbf{u}(\mathbf{x})]\,d\Gamma = 0 \tag{35}$$

$$\int_{\Gamma_I} \tilde{\mathbf{u}}^F(\mathbf{x}) \cdot [\sigma^F(\mathbf{x})\,\mathbf{n}_I(\mathbf{x}) + \mathbf{q}(\mathbf{x})]\,d\Gamma = 0. \tag{36}$$

The usual discretization is then introduced for all the boundary fields, i.e. displacements $\mathbf{u}$ and tractions $\mathbf{q}$ on $\overline{\Gamma}_B$, as well as for fictitious displacement discontinuities $\tilde{\mathbf{d}}$ and forces $\tilde{\mathbf{f}}$ on $\overline{\tilde{\Gamma}}_B$:

$$\mathbf{u}(\mathbf{x}) = \mathbf{N}_u(\mathbf{x})\mathbf{U}, \qquad \tilde{\mathbf{d}}(\tilde{\mathbf{x}}) = \mathbf{N}_u(\tilde{\mathbf{x}})\tilde{\mathbf{D}} \tag{37}$$

$$\mathbf{q}(\mathbf{x}) = \mathbf{N}_q(\mathbf{x})\mathbf{Q}, \qquad \tilde{\mathbf{f}}(\tilde{\mathbf{x}}) = \mathbf{N}_q(\tilde{\mathbf{x}})\tilde{\mathbf{F}} \tag{38}$$

Analogously the actual and auxiliary fields are discretized on Ω_F:

$$\mathbf{u}^F(\mathbf{x}) = \mathbf{N}_u^F(\mathbf{x})\mathbf{U}^F \qquad \tilde{\mathbf{u}}^F(\mathbf{x}) = \mathbf{N}_u^F(\mathbf{x})\tilde{\mathbf{U}}^F. \tag{39}$$

Exploiting eq. (35), the l.h.s. in eq. (26) can be given the form:

$$\frac{1}{2}\int_{\Gamma_I} \tilde{\mathbf{f}}(\mathbf{x}) \cdot \mathbf{u}(\mathbf{x})\,d\Gamma = \int_{\Gamma_I} \tilde{\mathbf{f}}(\mathbf{x}) \cdot \mathbf{u}^F(\mathbf{x})\,d\Gamma - \frac{1}{2}\int_{\Gamma_I} \tilde{\mathbf{f}}(\mathbf{x}) \cdot \mathbf{u}(\mathbf{x})\,d\Gamma.$$

The boundary equations (26), with the l.h.s. modified as above, as well as equations (27)-(29) are enforced in discretized form $\forall\tilde{\mathbf{F}}^I, \tilde{\mathbf{F}}^u, \tilde{\mathbf{D}}^I, \tilde{\mathbf{D}}^q$, so that their final versions give rise to the last four rows of the global equation system detailed in eq. (41).

With reference to FE subdomain, eq. (36) is introduced into (34); the resulting equation, also involving the unknown flux on Γ_I, reads:

$$\int_{\Omega_F} \tilde{\varepsilon}^F(\mathbf{x}) : \sigma^F(\mathbf{x})\,d\Omega + \int_{\Gamma_I} \tilde{\mathbf{u}}^F(\mathbf{x}) \cdot \mathbf{q}(\mathbf{x})\,d\Gamma = \int_{\Gamma_{Fq}} \tilde{\mathbf{u}}^F(\mathbf{x}) \cdot \overline{\mathbf{q}}(\mathbf{x})\,d\Gamma. \tag{40}$$

The discretized version of eq. (40), enforced $\forall\tilde{\mathbf{U}}^F$, represents the first row of the global equation system (41), which gathers all the BE and the FE equations:

$$\mathbf{M}\begin{Bmatrix} \mathbf{U}^F \\ \mathbf{Q}^I \\ \mathbf{Q}^u \\ \mathbf{U}^I \\ \mathbf{U}^q \end{Bmatrix} = \begin{Bmatrix} \overline{\mathbf{Q}}^F \\ \hat{\mathbf{G}}_{Iu}^{u\varphi}\overline{\mathbf{U}} + \mathbf{G}_{Iq}^{uu}\overline{\mathbf{Q}} \\ -\left(\frac{1}{2}\mathbf{I}_{uI}^t - \hat{\mathbf{G}}_{uu}^{u\varphi}\right)\overline{\mathbf{U}} + \mathbf{G}_{uq}^{uu}\overline{\mathbf{Q}} \\ \mathbf{G}_{Iu}^{\varphi\varphi}\overline{\mathbf{U}} + \hat{\mathbf{G}}_{Iq}^{\varphi u}\overline{\mathbf{Q}} \\ \mathbf{G}_{qu}^{\varphi\varphi}\overline{\mathbf{U}} + \left(\frac{1}{2}\mathbf{I}_{uI} + \hat{\mathbf{G}}_{qq}^{\varphi u}\right)\overline{\mathbf{Q}} \end{Bmatrix} \tag{41}$$

with $\mathbf{M}$ given by:

$$\mathbf{M} = \begin{bmatrix} \mathbf{K} & \mathbf{J}_{uI} & \mathbf{0} & \mathbf{0} & \mathbf{0} \\ \mathbf{J}_{uI}^t & -\mathbf{G}_{II}^{uu} & -\mathbf{G}_{Iu}^{uu} & -\frac{1}{2}\mathbf{I}_{uI}^t - \hat{\mathbf{G}}_{II}^{u\varphi} & -\hat{\mathbf{G}}_{Iq}^{u\varphi} \\ \mathbf{0} & -\mathbf{G}_{uI}^{uu} & -\mathbf{G}_{uu}^{uu} & -\hat{\mathbf{G}}_{uI}^{u\varphi} & -\hat{\mathbf{G}}_{uq}^{u\varphi} \\ \mathbf{0} & -\frac{1}{2}\mathbf{I}_{uI} - \hat{\mathbf{G}}_{II}^{\varphi u} & -\hat{\mathbf{G}}_{Iu}^{\varphi u} & -\mathbf{G}_{II}^{\varphi\varphi} & -\mathbf{G}_{Iq}^{\varphi\varphi} \\ \mathbf{0} & -\hat{\mathbf{G}}_{qI}^{\varphi u} & -\hat{\mathbf{G}}_{qu}^{\varphi u} & -\mathbf{G}_{qI}^{\varphi\varphi} & -\mathbf{G}_{qq}^{\varphi\varphi} \end{bmatrix}.$$

Note that $\mathbf{K}$ and $\overline{\mathbf{Q}}^F$ represent the FE stiffness matrix and the equivalent nodal loads; matrices $\mathbf{G}_{hk}^{ij}$ are defined analogously to the corresponding ones for the potential problem, for instance:

$$\mathbf{G}_{II}^{u\varphi} = \int_{\Gamma_I}\int_{\Gamma_I} \left[\mathbf{N}_q(\tilde{\mathbf{x}})\right]^t \mathbf{G}^{u\varphi}(\tilde{\mathbf{x}},\mathbf{x}) : \mathbf{R}[\mathbf{N}_u(\mathbf{x})]\,d\Gamma d\Gamma; \tag{42}$$

besides:

$$\hat{\mathbf{G}}_{hk}^{u\varphi} = \mathbf{G}_{hk}^{u\varphi} + \int_{\Gamma_{Bh}} \int_{\Gamma_{Bk}} \frac{\nabla r \cdot \mathbf{n}(\mathbf{x})}{4\pi r^2} \left[\mathbf{N}_q(\tilde{\mathbf{x}})\right]^t \mathbf{N}_u(\mathbf{x})\, d\Gamma d\tilde{\Gamma} \quad (43)$$

$$\hat{\mathbf{G}}_{hk}^{\varphi u} = \mathbf{G}_{hk}^{\varphi u} + \int_{\Gamma_{Bh}} \int_{\Gamma_{Bk}} \frac{\tilde{\nabla} r \cdot \tilde{\mathbf{n}}(\tilde{\mathbf{x}})}{4\pi r^2} \left[\mathbf{N}_u(\tilde{\mathbf{x}})\right]^t \mathbf{N}_q(\mathbf{x})\, d\Gamma d\tilde{\Gamma} \quad (44)$$

$$\mathbf{J}_{uI} = \int_{\Gamma_I} \left[\mathbf{N}_u^F(\mathbf{x})\right]^t \mathbf{N}_q(\mathbf{x})\, d\Gamma \quad (45)$$

$$\mathbf{I}_{uI} = \int_{\Gamma_I} \left[\mathbf{N}_u(\mathbf{x})\right]^t \mathbf{N}_q(\mathbf{x})\, d\Gamma. \quad (46)$$

Again, the symmetry of the coefficient matrix in the final equation system is ensured.

5 Formulation of the weak coupling procedure on a variational basis

The aim of this section is to show that the equations governing the coupled problem for the two subdomains Ω_F and Ω_B coincide with the set of stationarity conditions of an appropriate global functional. The approach to be followed, here described with reference to elasticity, parallels the ideas oulined in Bonnet (1995) for pure SGBEM equations, and differs from what developed in Polizzotto and Zito (1994) for a coupled SGBEM-FEM procedure.

With reference to the body $\Omega = \Omega_F \cup \Omega_B$ illustrated in the preceding section (under the assumption of no body forces), let us start introducing the FE subdomain potential energy:

$$\pi^F(\mathbf{u}^{\mathbf{F}}) = \int_{\Omega_F} \frac{1}{2} \nabla \mathbf{u}^{\mathbf{F}}(\mathbf{x}) : \mathbf{E} : \nabla \mathbf{u}^{\mathbf{F}}(\mathbf{x})\, d\Omega - \int_{\Gamma_{Fq}} \overline{\mathbf{q}}(\mathbf{x}) \cdot \mathbf{u}^{\mathbf{F}}(\mathbf{x})\, d\Gamma,$$

where $\mathbf{u}^{\mathbf{F}}$ satisfies the kinematical boundary conditions on Γ_{Fu}. As for the BE subdomain, an augmented potential energy is introduced

$$\pi^B(\mathbf{u}, \boldsymbol{\lambda}_1) = \int_{\Omega_B} \frac{1}{2} \nabla \mathbf{u}(\mathbf{x}) : \mathbf{E} : \nabla \mathbf{u}(\mathbf{x})\, d\Omega - \int_{\Gamma_{Bq}} \overline{\mathbf{q}}(\mathbf{x}) \cdot \mathbf{u}(\mathbf{x})\, d\Gamma - \int_{\Gamma_{Bu}} \boldsymbol{\lambda}_1(\mathbf{x}) \cdot [\mathbf{u}(\mathbf{x}) - \overline{\mathbf{u}}(\mathbf{x})]\, d\Gamma,$$

with displacements $\mathbf{u}$ unconstrained, in consequence of the introduction of the Lagrange multipliers $\boldsymbol{\lambda}_1$ for the kinematical boundary conditions on Γ_{Bu}. A global functional is built:

$$\pi(\mathbf{u}^{\mathbf{F}}, \mathbf{u}, \boldsymbol{\lambda}_1, \boldsymbol{\lambda}_2) = \pi^F(\mathbf{u}^{\mathbf{F}}) + \pi^B(\mathbf{u}, \boldsymbol{\lambda}_1) + \int_{\Gamma_I} \boldsymbol{\lambda}_2(\mathbf{x}) \cdot [\mathbf{u}^{\mathbf{F}}(\mathbf{x}) - \mathbf{u}(\mathbf{x})]\, d\Gamma. \quad (47)$$

Here $\boldsymbol{\lambda}_2$ are new Lagrange multipliers allowing the relaxation of the interface continuity conditions (i.e. $\mathbf{u}^{\mathbf{F}}$ and $\mathbf{u}$ are independent on Γ_I).

For the stationarity of functional π it is required that $\delta\pi(\mathbf{u}^{\mathbf{F}}, \mathbf{u}, \boldsymbol{\lambda}_1, \boldsymbol{\lambda}_2) = 0$, i.e.:

$$\begin{aligned} &\int_{\Omega_F} \nabla \mathbf{u}^{\mathbf{F}}(\mathbf{x}) : \mathbf{E} : \nabla \delta \mathbf{u}^{\mathbf{F}}(\mathbf{x})\, d\Omega - \int_{\Gamma_{Fq}} \overline{\mathbf{q}}(\mathbf{x}) \cdot \delta \mathbf{u}^{\mathbf{F}}(\mathbf{x})\, d\Gamma \\ &+ \int_{\Gamma_I} \boldsymbol{\lambda}_2(\mathbf{x}) \cdot \delta \mathbf{u}^{\mathbf{F}}(\mathbf{x})\, d\Gamma + \int_{\Omega_B} \nabla \mathbf{u}(\mathbf{x}) : \mathbf{E} : \nabla \delta \mathbf{u}(\mathbf{x})\, d\Omega \\ &- \int_{\Gamma_{Bq}} \overline{\mathbf{q}}(\mathbf{x}) \cdot \delta \mathbf{u}(\mathbf{x})\, d\Gamma - \int_{\Gamma_{Bu}} \boldsymbol{\lambda}_1(\mathbf{x}) \cdot \delta \mathbf{u}(\mathbf{x})\, d\Gamma \\ &- \int_{\Gamma_I} \boldsymbol{\lambda}_2(\mathbf{x}) \cdot \delta \mathbf{u}(\mathbf{x})\, d\Gamma - \int_{\Gamma_{Bu}} \delta \boldsymbol{\lambda}_1(\mathbf{x}) \cdot [\mathbf{u}(\mathbf{x}) - \overline{\mathbf{u}}(\mathbf{x})]\, d\Gamma \\ &+ \int_{\Gamma_I} \delta \boldsymbol{\lambda}_2(\mathbf{x}) \cdot [\mathbf{u}^{\mathbf{F}}(\mathbf{x}) - \mathbf{u}(\mathbf{x})]\, d\Gamma = 0. \end{aligned} \quad (48)$$

Using integration by parts and the divergence theorem, the domain integrals are transformed as follows (with the notation $\overline{\Gamma}_F = \Gamma_F \cup \Gamma_I$):

$$\int_{\Omega_F} \nabla \mathbf{u}^{\mathbf{F}}(\mathbf{x}) : \mathbf{E} : \nabla \delta \mathbf{u}^{\mathbf{F}}(\mathbf{x})\, d\Omega = \int_{\overline{\Gamma}_F} \delta \mathbf{u}^{\mathbf{F}}(\mathbf{x}) \cdot \boldsymbol{\sigma}^F(\mathbf{x})\, \mathbf{n}(\mathbf{x}) d\Gamma - \int_{\Omega_F} \delta \mathbf{u}^{\mathbf{F}}(\mathbf{x}) \cdot \mathrm{div}[\boldsymbol{\sigma}^F(\mathbf{x})]\, d\Omega$$

$$\int_{\Omega_B} \nabla \mathbf{u}(\mathbf{x}) : \mathbf{E} : \nabla \delta \mathbf{u}(\mathbf{x})\, d\Omega = \int_{\overline{\Gamma}_B} \delta \mathbf{u}(\mathbf{x}) \cdot \mathbf{q}(\mathbf{x}) d\Gamma - \int_{\Omega_B} \delta \mathbf{u}(\mathbf{x}) \cdot \mathrm{div}[\boldsymbol{\sigma}(\mathbf{x})]\, d\Omega.$$

If the latter conditions are introduced into eq. (48), taking into account that $\delta \mathbf{u}^{\mathbf{F}}(\mathbf{x}) = 0$ along Γ_{Fu}, in view of the

arbitrariness of the variations the following relations are obtained for the FE subdomain:

$$\begin{aligned}&\operatorname{div}[\sigma^F(\mathbf{x})] = 0 \ \text{ in } \Omega_F,\\ &\sigma^F(\mathbf{x})\,\mathbf{n}(\mathbf{x}) = \overline{\mathbf{q}}(\mathbf{x}) \ \text{ along } \Gamma_{Fq}\end{aligned}$$

and for the BE subdomain:

$$\begin{aligned}&\operatorname{div}[\sigma(\mathbf{x})] = 0 \ \text{ in } \Omega_B,\\ &\mathbf{q}(\mathbf{x}) = \overline{\mathbf{q}}(\mathbf{x}) \ \text{ along } \Gamma_{Bq},\\ &\mathbf{q}(\mathbf{x}) = \lambda_{\mathbf{1}}(\mathbf{x}), \quad \mathbf{u}(\mathbf{x}) = \overline{\mathbf{u}}(\mathbf{x}) \ \text{ along } \Gamma_{Bu}\end{aligned}$$

with interface conditions:

$$\begin{aligned}&\mathbf{u}^{\mathbf{F}}(\mathbf{x}) = \mathbf{u}(\mathbf{x}),\\ &\sigma^F(\mathbf{x})\,\mathbf{n}_I(\mathbf{x}) = -\lambda_{\mathbf{2}}(\mathbf{x}), \quad \mathbf{q}(\mathbf{x}) = \lambda_{\mathbf{2}}(\mathbf{x})\end{aligned} \qquad \text{along } \Gamma_I.$$

Hence the Lagrange multipliers $\lambda_{\mathbf{1}}$ and $\lambda_{\mathbf{2}}$ coincide with the BE tractions on Γ_{Bu} and Γ_I respectively; obviously the two latter conditions along Γ_I imply that $\sigma^F(\mathbf{x})\,\mathbf{n}_I(\mathbf{x}) = -\mathbf{q}(\mathbf{x})$. Thus the stationarity of functional $\pi(\mathbf{u}^{\mathbf{F}}, \mathbf{u}, \lambda_{\mathbf{1}}, \lambda_{\mathbf{2}})$ leads to the whole set of equations which govern the coupled elastic problem on $\Omega = \Omega_F \cup \Omega_B$ and the converse can also be proved easily.

Now we intend to show that if the independent variations are suitably selected, all the equations leading, after discretization, to system (41) can be obtained as stationarity conditions of fuctional π. Exploiting the arbitrariness of the variations, first all the contributions involving $\delta\mathbf{u}^{\mathbf{F}}$ in eq. (48) are gathered (setting $\delta\mathbf{u}^{\mathbf{F}} \neq 0$, $\delta\mathbf{u} = \delta\lambda_{\mathbf{1}} = \delta\lambda_{\mathbf{2}} = 0$):

$$\begin{aligned}&\int_{\Omega_F} \nabla\mathbf{u}^{\mathbf{F}}(\mathbf{x}) : \mathbf{E} : \nabla\delta\mathbf{u}^{\mathbf{F}}(\mathbf{x})\,d\Omega - \int_{\Gamma_{Fq}} \overline{\mathbf{q}}(\mathbf{x}) \cdot \delta\mathbf{u}^{\mathbf{F}}(\mathbf{x})\,d\Gamma\\ &\quad + \int_{\Gamma_I} \lambda_{\mathbf{2}}(\mathbf{x}) \cdot \delta\mathbf{u}^{\mathbf{F}}(\mathbf{x})\,d\Gamma = 0.\end{aligned} \tag{49}$$

When π is stationary, $\lambda_{\mathbf{2}}(\mathbf{x}) = \mathbf{q}(\mathbf{x})$ along Γ_I, thus eq. (49) is recognized to be the FE subdomain equation, eq. (40), involved by the proposed coupling procedure. Then all the complementary terms in eq. (48) are taken into account (setting $\delta\mathbf{u}^{\mathbf{F}} = 0$, $\delta\mathbf{u} \neq 0$, $\delta\lambda_{\mathbf{1}} \neq 0$, $\delta\lambda_{\mathbf{2}} \neq 0$):

$$\begin{aligned}&\int_{\Omega_B} \nabla\mathbf{u}(\mathbf{x}) : \mathbf{E} : \nabla\delta\mathbf{u}(\mathbf{x})\,d\Omega - \int_{\Gamma_{Bq}} \overline{\mathbf{q}}(\mathbf{x}) \cdot \delta\mathbf{u}(\mathbf{x})\,d\Gamma\\ &\quad - \int_{\Gamma_{Bu}} \lambda_{\mathbf{1}}(\mathbf{x}) \cdot \delta\mathbf{u}(\mathbf{x})\,d\Gamma - \int_{\Gamma_I} \lambda_{\mathbf{2}}(\mathbf{x}) \cdot \delta\mathbf{u}(\mathbf{x})\,d\Gamma\\ &\quad - \int_{\Gamma_{Bu}} \delta\lambda_{\mathbf{1}}(\mathbf{x}) \cdot [\mathbf{u}(\mathbf{x}) - \overline{\mathbf{u}}(\mathbf{x})]\,d\Gamma\\ &\quad + \int_{\Gamma_I} \delta\lambda_{\mathbf{2}}(\mathbf{x}) \cdot [\mathbf{u}^{\mathbf{F}}(\mathbf{x}) - \mathbf{u}(\mathbf{x})]\,d\Gamma = 0.\end{aligned} \tag{50}$$

The domain integral in eq. (50) is manipulated analogously as before, but integration by parts is now applied as follows:

$$\begin{aligned}&\int_{\Omega_B} \nabla\mathbf{u}(\mathbf{x}) : \mathbf{E} : \nabla\delta\mathbf{u}(\mathbf{x})\,d\Omega = \int_{\overline{\Gamma}_B} \mathbf{u}(\mathbf{x}) \cdot \delta\mathbf{q}^u(\mathbf{x})\,d\Gamma\\ &\quad - \int_{\Omega_B} \mathbf{u}(\mathbf{x}) \cdot \operatorname{div}[\delta\sigma^u(\mathbf{x})]\,d\Omega.\end{aligned}$$

Here the following notation has been introduced:

$$\delta\mathbf{q}^u(\mathbf{x}) = \delta\sigma^u(\mathbf{x})\,\mathbf{n}(\mathbf{x}) = [\mathbf{E} : \nabla\delta\mathbf{u}(\mathbf{x})]\,\mathbf{n}(\mathbf{x}),$$

thus $\delta\mathbf{q}^u(\mathbf{x})$ and $\delta\sigma^u(\mathbf{x})$ represent tractions and stresses related via constitutive relations to $\delta\mathbf{u}(\mathbf{x})$ respectively. For an elastic body in equilibrium with zero body forces variations, $\operatorname{div}[\delta\sigma^u(\mathbf{x})] = 0$, thus the domain integral in the r.h.s. of the last equation vanishes. With the further assumption

$$\delta\lambda_{\mathbf{1}}(\mathbf{x}) = \delta\mathbf{q}^u(\mathbf{x}) \quad \text{along } \Gamma_{Bu}, \tag{51}$$

eq. (50) can be written as:

$$\begin{aligned}&\int_{\Gamma_{Bq}} [\mathbf{u}(\mathbf{x}) \cdot \delta\mathbf{q}^u(\mathbf{x}) - \overline{\mathbf{q}}(\mathbf{x}) \cdot \delta\mathbf{u}(\mathbf{x})]d\Gamma\\ &\quad + \int_{\Gamma_{Bu}} [\overline{\mathbf{u}}(\mathbf{x}) \cdot \delta\mathbf{q}^u(\mathbf{x}) - \lambda_{\mathbf{1}}(\mathbf{x}) \cdot \delta\mathbf{u}(\mathbf{x})]\,d\Gamma\\ &\quad + \int_{\Gamma_I} [\mathbf{u}(\mathbf{x}) \cdot \delta\mathbf{q}^u(\mathbf{x}) - \lambda_{\mathbf{2}}(\mathbf{x}) \cdot \delta\mathbf{u}(\mathbf{x})]\,d\Gamma\\ &\quad + \int_{\Gamma_I} \delta\lambda_{\mathbf{2}}(\mathbf{x}) \cdot [\mathbf{u}^{\mathbf{F}}(\mathbf{x}) - \mathbf{u}(\mathbf{x})]\,d\Gamma = 0.\end{aligned} \tag{52}$$

The way to build the test function $\delta\mathbf{u}(\mathbf{x})$ represents a crucial point: the potential theory states that any displacement field such that $\mathrm{div}[\delta\sigma^u(\mathbf{x})] = 0$ admits an integral representation; following Bonnet (1995), the following integral representation is assumed:

$$\delta\mathbf{u}(\mathbf{x}) = \int_{\tilde{\Gamma}_{Bq}\cup\tilde{\Gamma}_I} \mathbf{G}^{uq}(\mathbf{x},\tilde{\mathbf{x}})\,\tilde{\mathbf{d}}(\tilde{\mathbf{x}})\,d\tilde{\Gamma} - \int_{\tilde{\Gamma}_{Bu}\cup\tilde{\Gamma}_I} \mathbf{G}^{uu}(\mathbf{x},\tilde{\mathbf{x}})\,\tilde{\mathbf{f}}(\tilde{\mathbf{x}})\,d\tilde{\Gamma}. \quad (53)$$

which implies the following traction representation:

$$\delta\mathbf{q}^u(\mathbf{x}) = \int_{\tilde{\Gamma}_{Bq}\cup\tilde{\Gamma}_I} \mathbf{G}^{qq}(\mathbf{x},\tilde{\mathbf{x}})\,\tilde{\mathbf{d}}(\tilde{\mathbf{x}})\,d\tilde{\Gamma} - \int_{\tilde{\Gamma}_{Bu}\cup\tilde{\Gamma}_I} \mathbf{G}^{qu}(\mathbf{x},\tilde{\mathbf{x}})\,\tilde{\mathbf{f}}(\tilde{\mathbf{x}})\,d\tilde{\Gamma}. \quad (54)$$

The two auxiliary functions, $\tilde{\mathbf{d}}(\tilde{\mathbf{x}})$ and $\tilde{\mathbf{f}}(\tilde{\mathbf{x}})$, appearing in eq. (53) and eq. (54), represent variations of displacement and traction jumps respectively across a surface $\tilde{\overline{\Gamma}}_B$ exterior to $\overline{\Gamma}_B$, (points belonging to these two surfaces are in a one-to-one correspondence). The following choice is also made: $\tilde{\mathbf{d}}(\tilde{\mathbf{x}}) = \mathbf{0}$ over $\tilde{\Gamma}_{Bu}$ and $\tilde{\mathbf{f}}(\tilde{\mathbf{x}}) = \mathbf{0}$ over $\tilde{\Gamma}_{Bq}$. Having selected the variations $\delta\mathbf{u}$ and $\delta\lambda_1$ according to eq. (53) and eq. (51), eq. (52) is enforced for any $\tilde{\mathbf{d}}$ along $\tilde{\Gamma}_{Bq}$ and $\tilde{\Gamma}_I$ and for any $\tilde{\mathbf{f}}$ along $\tilde{\Gamma}_{Bu}$ respectively. Exploiting the reciprocity properties of the fundamental solutions, detailed i.e. in Sirtori, Maier, Novati and Miccoli (1992), preliminary versions (in the sense that surfaces $\tilde{\overline{\Gamma}}_B$ and $\overline{\Gamma}_B$ are still distinct) of eqs. (27)-(29) can be derived: traction equations on Γ_{Bq} and on Γ_I, displacement equation on Γ_{Bu}. Setting to zero $\tilde{\mathbf{d}}$ along $\tilde{\Gamma}_{Bq}$ and $\tilde{\Gamma}_I$ and $\tilde{\mathbf{f}}$ along $\tilde{\Gamma}_{Bu}$, eq. (52) reduces to:

$$\int_{\tilde{\Gamma}_I} \tilde{\mathbf{f}}(\tilde{\mathbf{x}}) \cdot \left[\int_{\overline{\Gamma}_B} \left[\mathbf{G}^{uu}(\tilde{\mathbf{x}},\mathbf{x})\,\mathbf{q}(\mathbf{x}) - \mathbf{G}^{uq}(\tilde{\mathbf{x}},\mathbf{x})\,\mathbf{u}(\mathbf{x}) \right] d\Gamma \right] d\tilde{\Gamma} + \int_{\Gamma_I} \delta\boldsymbol{\lambda}_{\mathbf{2}}(\mathbf{x}) \cdot \left[\mathbf{u}^{\mathbf{F}}(\mathbf{x}) - \mathbf{u}(\mathbf{x}) \right] d\Gamma = 0 \quad (55)$$

where $\mathbf{q}(\mathbf{x}) = \overline{\mathbf{q}}(\mathbf{x})$ along Γ_{Bq}, $\mathbf{u}(\mathbf{x}) = \overline{\mathbf{u}}(\mathbf{x})$ along Γ_{Bu} and $\mathbf{q}(\mathbf{x}) = \lambda_2(\mathbf{x})$ along Γ_I.

Through a regularization of the singular kernels (here the one detailed in Frangi, Novati, Springhetti and Rovizzi (2002) has been adopted), the limit process for $\tilde{\overline{\Gamma}}_B \to \overline{\Gamma}_B$ can be performed and eqs. (27)-(29) are obtained. Variation $\delta\boldsymbol{\lambda}_{\mathbf{2}}(\mathbf{x})$ along Γ_I is chosen as follows:

$$\delta\boldsymbol{\lambda}_{\mathbf{2}}(\mathbf{x}) = -\,\tilde{\mathbf{f}}(\mathbf{x}), \quad (56)$$

so that eq. (55) reads:

$$\int_{\Gamma_I} \tilde{\mathbf{f}}(\mathbf{x}) \cdot \mathbf{u}^F(\mathbf{x})\,d\Gamma - \frac{1}{2}\int_{\Gamma_I} \tilde{\mathbf{f}}(\mathbf{x}) \cdot \mathbf{u}(\mathbf{x})\,d\Gamma = \int_{\Gamma_I} \tilde{\mathbf{f}}(\tilde{\mathbf{x}}) \cdot \int_{\overline{\Gamma}_B} \Big[\mathbf{G}^{uu}(\tilde{\mathbf{x}},\mathbf{x})\,\mathbf{q}(\mathbf{x}) + \frac{\nabla r \cdot \mathbf{n}(\mathbf{x})}{4\pi r^2}\mathbf{u}(\mathbf{x}) + \mathbf{G}^{u\varphi}(\tilde{\mathbf{x}},\mathbf{x}) : \mathbf{R}[\mathbf{u}](\mathbf{x}) \Big] d\Gamma d\Gamma. \quad (57)$$

This is recognized to be the modified version of eq. (26) involved in the coupling procedure, i.e. the equation which, after discretization, gives rise to the second row of the final equation system (41). Thus all the equations used in the SGBEM-FEM coupling procedure have been shown to stem from a variational approach based on an augmented potential energy functional.

6 Numerical examples: 3D elastoplasticity

The weak SGBEM-FEM coupling scheme developed in Section 4 for elasticity has been implemented into a step-by-step procedure for elastoplastic evolutive analysis. Elastoplastic problems with limited spread of plastic strains lend themselves to a coupled approach: FE equations are adopted over the region where plasticity is bound to develop (with enforcement of the constitutive law at Gauss points), while BE equations are written over the complementary elastic region. Here an elastic-perfectly plastic material obeying the von Mises yield criterion has been considered with an associated flow rule. The global equation system (41), in incremental form, is solved at each iteration within a load step using a tangent FE stiffness matrix $\mathbf{K}$ (see e.g. Simo and Hughes (1998) for further details on computational aspects).

Two numerical examples are presented hereafter. In view of the adopted weak enforcement of the transmission conditions on Γ_I, the BE and the FE mesh do not need to satisfy any matching condition at the interface. Quadratic isoparametric FEs and BEs are used for both examples.

6.1 Thick hollow sphere under internal pressure

The pressurized thick-walled elastic-plastic spherical shell depicted in Fig. 5 is addressed; the problem, characterized by spherical symmetry, admits an explicit analytic solution, see for instance Lubliner (1990).

The shell has inner and outer radius of $100\,mm$ and $300\,mm$, respectively, and the material elastic moduli are

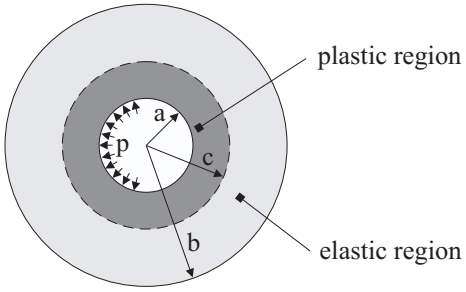

Figure 5 : Pressurized thick hollow sphere: elastic-plastic behavior

$E = 206 \cdot 10^3 MPa$, $\nu = 0.3$, while the yield stress is $\sigma_y = 360 MPa$. Two different meshes illustrated in Fig. 6

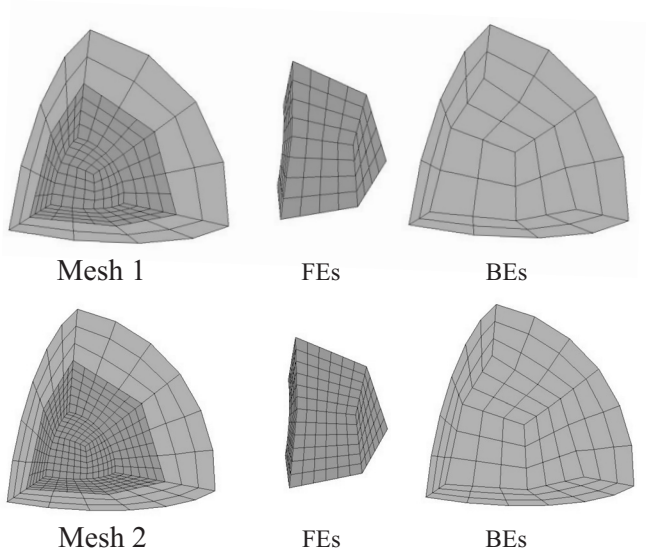

Figure 6 : Meshes 1, 2 and the model for the interface

have been used (for symmetry reasons only one eighth of the whole sphere has been analyzed), with a piecewise plane interface Γ_I:

- mesh 1: 1235 nodes, 3462 degrees of freedom, with 48 BEs and 192 FEs;
- mesh 2: 3615 nodes, 10347 degrees of freedom, with 108 BEs and 648 FEs.

Hexaedral FEs extend from the inner surface, $r = a$, to Γ_I, while quadrilateral BEs are used for the outer portion. The internal pressure is increased from zero to $500 MPa$; for this load, the elastic-plastic interface ($c = 149.54 mm$) lies inside Ω_F. Fig. 7 and Fig. 8 show the numerical results in terms of radial displacement and von Mises equivalent stress (the latter through the thickness of the FE subdomain).

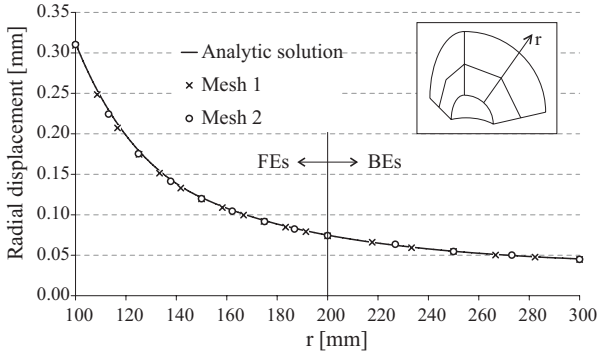

Figure 7 : Displacement along the radius shown in the inset for $p = 500 MPa$

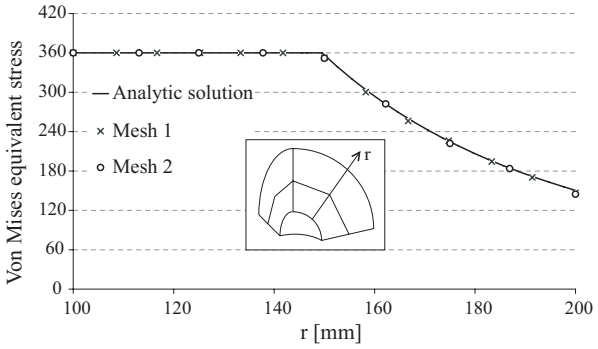

Figure 8 : von Mises equivalent stress (FE subdomain) for $p = 500 MPa$

6.2 Simply supported notched beam

As second example, the simply supported notched beam of Fig. 9 is considered; the geometry of the notch is shown in Fig. 10 (all lengths are expressed in *mm*).

As in the preceding example, the material is characterized by: $E = 206 \cdot 10^3 MPa$, $\nu = 0.3$ and $\sigma_y = 360 MPa$. Since no analytic solution is available for this example, a numerical reference solution is generated by means of a commercial FE package (Ansys 9.0) utilizing a very fine mesh (85844 nodes, 19540 hexaedral quadratic elements, 255528 degrees of freedom) for the discretization of one half of the beam. It turns out that the first yielding takes

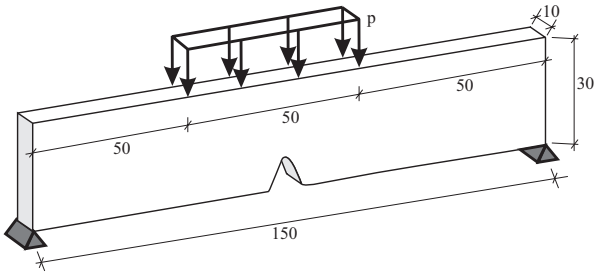

Figure 9 : Notched beam geometry

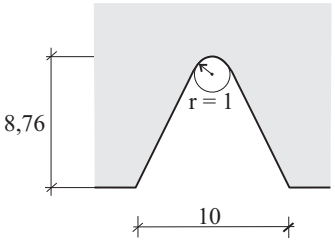

Figure 10 : Detail of the notch

place at the notch for a load of about $8\,MPa$; as the load grows, plasticity develops first around the notch and, for higher load levels, also in the region below the applied load; the limit load is around $30.5\,MPa$. The two BE and

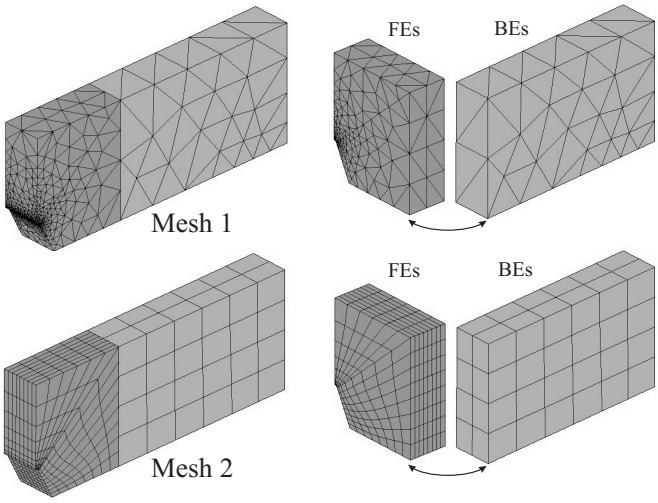

Figure 11 : Meshes 1, 2 and detail of the interface

FE meshes used in the analysis with the coupling procedure are depicted in Fig. 11 and are characterized by:

- mesh 1: 7362 nodes and 21387 degrees of freedom, pertaining to 122 triangular BEs and 4144 tetrahedral FEs;
- mesh 2: 4775 nodes and 14211 degrees of freedom, pertaining to 88 quadrilateral BEs and 896 hexaedral FEs.

In both cases the interface Γ_I is a plane surface.

The overall behavior of the beam is represented by the load-displacement curve of Fig. 12: the good agreement between the FE reference solution and the SGBEM-FEM solutions is evidenced. For $p = 27MPa$ a comparison of vertical displacement along the upper edge of the beam is shown in Fig. 13; the percentage error in terms of the maximum displacement is less than 2.4% and 1.6% for mesh1 and mesh 2, respectively. For the same load level, the von Mises equivalent stress obtained in the reference solution and using the SGBEM-FEM technique is represented by contour maps in Fig. 14 and Figs. 15-16, respectively.

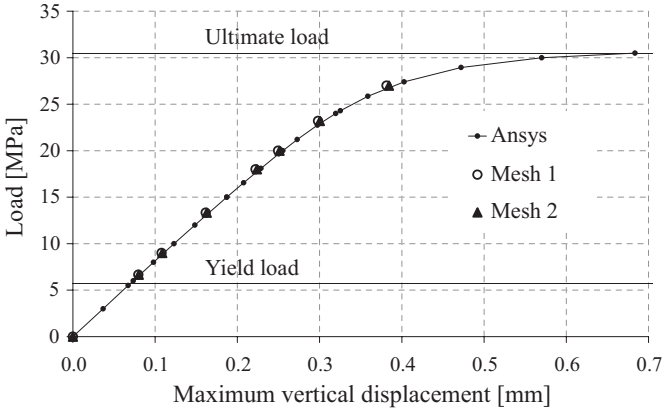

Figure 12 : Load vs. maximum vertical displacement

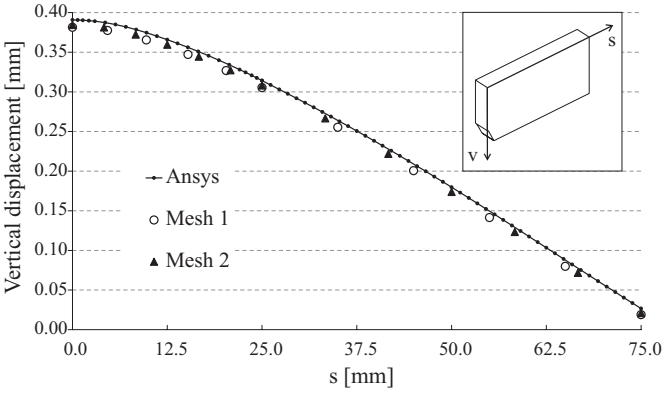

Figure 13 : Comparison between vertical displacements ($p = 27$ MPa)

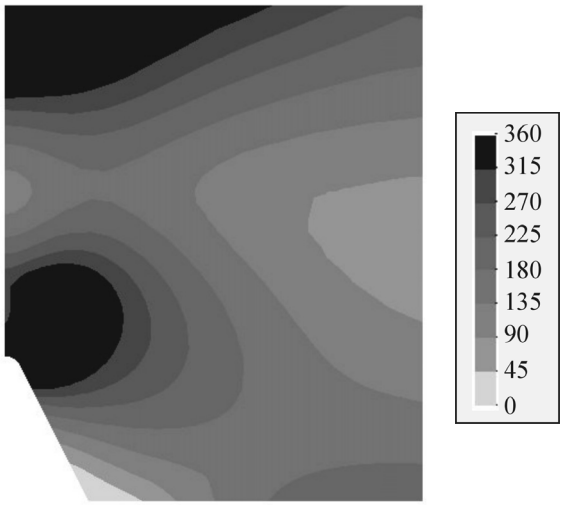

Figure 14 : Numerical reference solution: von Mises equivalent stress ($p = 27$ MPa)

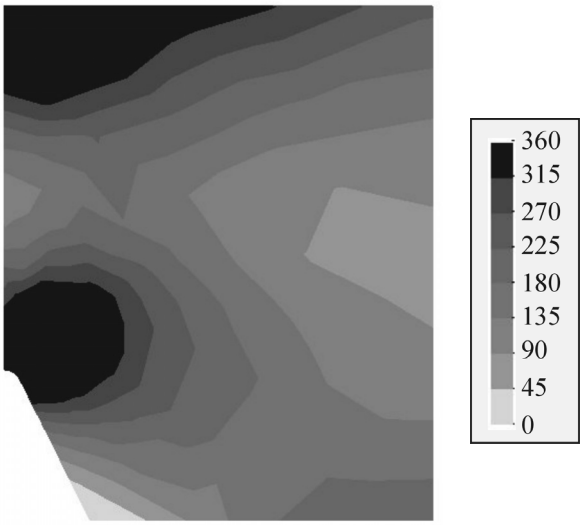

Figure 15 : SGBEM-FEM mesh 1: von Mises stress ($p = 27$ MPa)

7 Conclusions

A procedure for a weak coupling between SGBEM and FEM is presented, both for 2D potential problems and 3D elasticity; a fully symmetric global coefficient matrix is directly generated. The procedure allows to adopt a completely independent modeling of the FE and BE subdomains: no matching of the nodes is required on the interface; this allows a greater flexibility in the modeling, which can be useful in various contexts. A computer code has been implemented for both potential 2D problems and elastoplastic 3D problems with material nonlinearity confined to the FE subdomain. The numerical results confirm the effectiveness of the proposed procedure.

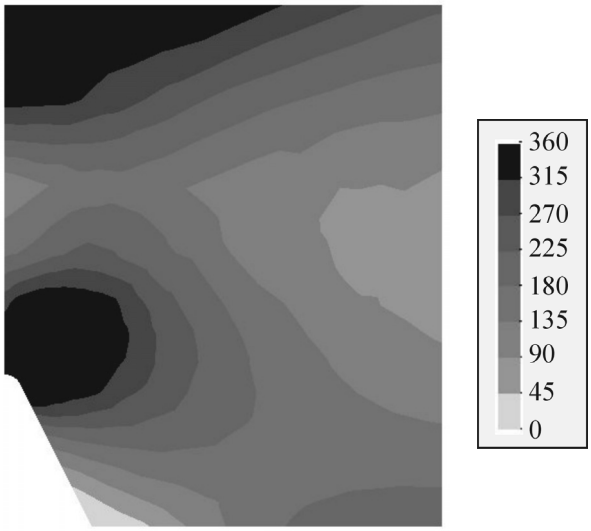

Figure 16 : SGBEM-FEM mesh 2: von Mises stress ($p = 27$ MPa)

Acknowledgement: The present work has been carried out within a research project funded by the Italian Ministry for University and Research (MIUR, Prin 2004).

References

Bonnet M. (1995): Regularized direct and indirect symmetric variational BIE formulations for three-dimensional elasticity. *Eng. Anal. Bound. Elem.*, vol. 15, pp. 93-102.

Bonnet M.; Maier G.; Polizzotto C. (1998): Symmetric Galerkin boundary element method. *Appl. Mech. Rev.*, vol. 51, no. 11, pp. 669-704.

Elleithy W.M.; Tanaka M. (2003): Interface relaxation algorithms for BEM-BEM coupling and FEM-BEM coupling. *Comput. Meth. Appl. Mech. Engng.*, vol. 192, pp. 2977-2992.

Forth S.C.; Staroselsky A. (2005): A hybrid FEM/BEM approach for designing an aircraft engine structural

health monitoring. *CMES: Computer Modeling in Engineering & Sciences*, vol. 9, no. 3, pp. 287-298.

Frangi A.; Novati G.; Springhetti R.; Rovizzi M. (2002): 3D fracture analysis by the symmetric Galerkin BEM. *Comput. Mech.*, vol. 28, pp. 220-232.

Frangi A.; Novati G. (2003): BEM-FEM coupling for 3D fracture mechanics applications. *Comput. Mech.*, vol. 32, pp. 415-422.

Ganguly S.; Layton J.B.; Balakrishna C. (2000): Symmetric coupling of multi-zone curved Galerkin boundary elements with finite elements in elasticity. *Int. J. Numer. Meth. Engng.*, vol. 48, pp. 633-654.

Ganguly S.; Layton J.B.; Balakrishna C. (2004): A coupling of multi-zone curved Galerkin BEM with finite elements for independently modelled sub-domains with non-matching nodes in elasticity. *Int. J. Numer. Meth. Engng.*, vol. 59, pp. 1021-1038.

Haas M.; Kuhn G. (2003): Mixed-dimensional, symmetric coupling of FEM and BEM. *Eng. Anal. Bound. Elem.*, vol. 27, pp. 575-582.

Han Z.D.; Atluri S.N. (2002): SGBEM (for cracked local subdomain) - FEM (for uncracked global structure) alternating method for analyzing 3D surface cracks and their fatigue-growth. *CMES: Computer Modeling in Engineering & Sciences*, vol. 3, no. 6, pp. 699-716.

Han Z.D.; Atluri S.N. (2003): On simple formulations of weakly-singular traction & displacement BIE, and their solutions through Petrov-Galerkin approaches. *CMES: Computer Modeling in Engineering & Sciences*, vol. 4, no. 1, pp. 5-20.

Keat W.D.; Annigeri B.S.; Cleary M.P. (1988): Surface integral and finite element hybrid method for two and three dimensional fracture mechanics analysis. *Int. J. Fract.*, vol. 36, pp. 35-53.

Li S.; Mear M.E.; Xiao L. (1998): A hybrid coupled finite-boundary element method in elasticity. *Comput. Meth. Appl. Mech. Engng.*, vol. 151, no. 3-4, pp. 435-459.

Lubliner J. (1990): *Plasticity theory*, Macmillan Publishing Company.

Polizzotto C.; Zito M. (1994): Variational formulations for coupled BE/FE methods in elastostatics. *ZAMM*, vol. 74, pp. 533-543.

Sauter S.A.; Schwab C. (1997): Quadrature for hp-Galerkin BEM in 3-d. *Num. Math.*, vol. 78, pp. 211-258.

Simo J.C.; Hughes T.J.R. (1998): *Computational inelasticity*, Springer, ed. Marsden, Wiggins, Sirovich.

Sirtori S.; Maier G.; Novati G.; Miccoli S. (1992): A Galerkin symmetric boundary-element method in elasticity: formulation and implementation. *Int. J. Numer. Meth. Engng.*, vol. 35, pp. 255-282.

Zienkiewicz O.C.; Kelly D.W.; Bettes P. (1977): The coupling of the finite elements and boundary solution procedures. *Int. J. Numer. Meth. Engng.*, vol. 11, pp. 355-375.